

A Versatile Approach to the Synthesis of Functionalized Thiol-Protected Palladium Nanoparticles

Matteo Cargnello,[†] Noah L. Wieder,[‡] Patrizia Canton,[§] Tiziano Montini,[†] Giuliano Giambastiani,[∞] Alvise Benedetti,[§] Raymond J. Gorte,[‡] and Paolo Fornasiero^{*,†}

[†]Department of Chemical and Pharmaceutical Sciences, ICCOM-CNR, INSTM, Center of Excellence for Nanostructured Materials (CENMAT), University of Trieste, Via L. Giorgieri 1, 34127 Trieste, Italy

[‡]Department of Chemical and Biomolecular Engineering, University of Pennsylvania, 311A Towne Building, 220 South 33rd Street, Philadelphia, Pennsylvania 19104, United States

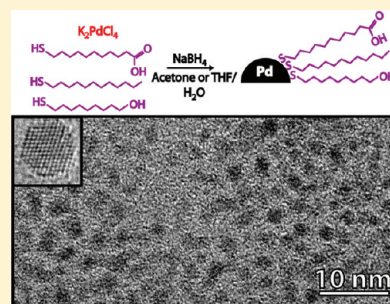
[§]Department of Molecular Science and Nanosystems, Università Ca' Foscari Venezia, Via Torino 155/B, 30172 Venice, Italy

[∞]Istituto di Chimica dei Composti Organometallici (ICCOM-CNR), Via Madonna del Piano 10, 50019—Sesto Fiorentino (Firenze), Italy

S Supporting Information

ABSTRACT: A synthesis of variably functionalized thiol-protected palladium nanoparticles (Pd-NPs) is presented. The nanoparticle syntheses are performed in acetone–water or tetrahydrofuran–water solutions, without making use of either phase-transfer agents or complex purification procedures of the as-synthesized nanoparticles. Small and mostly monodisperse thiol-protected Pd nanoparticles (Pd-NPs ~ 2 nm) have been prepared with 11-mercaptopundecanoic acid (MUA), 9-mercapto-1-nonanol (MN), 1-dodecanethiol (DT), or mixtures thereof, and a simple scale-up synthesis is also proposed. The role of Pd^{II}-thiolate species as metal precursors in the stage of nanoparticle synthesis and the influence of the reaction parameters on the final Pd-NPs size and size distribution are discussed. The formation of mixed-monolayer protected nanoparticles is achieved, with the final monolayer composition dictated by the thiols, initial molar ratio. Overall, the procedure presented here allows the preparation of functionalized nanoparticles with a high density of functional groups at the edge of the monolayer, with no need of place-exchange reactions. Specific postfunctionalization procedures conducted at the acid groups of the MUA-Pd monolayer are reported so as to widen the potential applicability of these amphiphilic nanoparticle precursors with respect to different applications in the field of material science. Finally, the successful use and the easy recycling/reuse of the Pd-NPs in a model Suzuki cross-coupling reaction are presented.

KEYWORDS: palladium nanoparticles, thiols, amphiphilic NPs, self-assembled monolayers, mixed monolayers



1. INTRODUCTION

The preparation of monolayer-protected clusters (MPCs) had a significant impact in chemistry, physics, and materials science.^{1–3} On this basis, Au–thiol systems are rapidly emerged as systems of particular interest due to the high chemical stability of the Au–S bond.²

Although less investigated, thiol-protected nanoparticles based on other noble metals, such as Pd, Pt, or Ir are expected to have very different properties, besides showing important applications in electron transfer processes and in photochemical and electronic devices.⁴

While the synthesis of mostly monodisperse nanoparticles (NPs) is nowadays well-established (particularly in the case of Au),⁵ severe limitations to bringing different functionalities on the nanoparticle board (particularly those sensitive to reducing agents)^{6,7} are still present. One of the most common methods to bring functional groups on Au nanoparticles involves an exchange reaction between the pre-existing thiols in the self-assembled monolayer (SAM) surrounding the preformed

nanoparticles and other added thiols.⁸ Although this method has some advantages, the achievement of a high functional group density at the edge of the monolayer is rather difficult, due to the equilibrium character of the “place-exchange” reaction.⁹ Other methods have been successfully developed under milder reducing conditions, in all cases leading to average particle sizes larger than 3 nm,^{10,11} with limited applicability in catalysis.¹²

In this paper we report on a convenient approach for the preparation of thiol-protected Pd nanoparticles capped by either 11-mercaptopundecanoic acid (MUA) or 9-mercapto-1-nonanol (MN) or 1-dodecanethiol (DT) or mixtures thereof. Although one-phase¹³ and two-phase¹⁴ procedures for the synthesis of thiol-protected Pd nanoparticles have already been reported, the use of either strong reducing agents (such as LiBEt₃H) or costly and time-consuming thiol

Received: May 24, 2011

Published: August 09, 2011

exchange protocols still represent a major drawback in the preparation of highly functionalized Pd-NP SAMs.

The procedure described here represents a significant improvement with respect to what has been recently reported by some of us¹⁵ and allows for the simple preparation of nanoparticles having high densities of either COOH or OH functionalities at their surface. Furthermore, the functional group density can be easily tuned by using mixtures of thiols in combination with 1-dodecanethiol, resulting in tailor-made protected clusters whose SAM composition is dictated by the initial thiol mixture molar ratio. Accordingly, small metal-core Pd nanoparticles have been prepared using a method that combines the positive features of the Brust–Schiffman protocol⁶ with those of a single-phase synthesis.¹⁶ Moreover, the use of MUA as protecting thiol has led to the obtainment of amphiphilic Pd nanoparticles. The latter show increased solubility within different media, thus avoiding the use of phase transfer agents. Indeed, the long MUA alkyl chains ensure solubility of the NPs in polar and apolar organic solvents, while solubility in water is simply achieved once the carboxylic groups are converted into their carboxylate forms (11-mercaptopundecanoate, MUAt). High water solubility of the Pd-NPs (like our MUAt-Pd NPs) makes them potentially attractive for biological applications. Most importantly, this wide solubility range strictly correlates to both the small metal-core particle size and the high density of the functional groups at the edge of the SAM.

Simple postfunctionalization procedures on the carboxylic acid at the edge of the SAM in the MUA-Pd nanoparticles have also been successfully addressed. Such results set the way for the design and synthesis of more complex, core–shell systems of potential interest in electrochemical, photochemical, and photophysical fields.

Although water-soluble thiol-protected Au and Pd nanoparticles have already been reported by other groups using a number of different compounds (tiopronin,¹⁷ mercaptoammonium thiols,¹⁸ poly(ethyleneglycol)-alkyl thiols,¹⁹ mercaptosuccinic acid²⁰), there are few examples of amphiphilic thiol-protected Pd particles and their convenient use in catalysis.²¹

2. EXPERIMENTAL SECTION

2.1. General Considerations and Materials. Potassium tetrachloropalladate(II) (32.04% as Pd) was purchased from ChemPur. 11-Mercaptopundecanoic acid (MUA, 95%), 9-mercapto-1-nonanol (MN, 96%), 1-dodecanethiol (DT, $\geq 98\%$), (benzotriazol-1-yloxy)tris-(dimethylamino)phosphonium hexafluorophosphate (BOP, 97%), and 1-hydroxybenzotriazole hydrate (HOBt, $\geq 97\%$) were purchased from Sigma-Aldrich and used as received. Solvents (reagent grade), including deuterated solvents, were purchased from Sigma-Aldrich and used as received. ¹H NMR spectra were recorded on a JEOL GX-400 MHz (operating at 400 MHz for ¹H) using methanol-*d*₄, CDCl₃, or acetone-*d*₆ as solvents. Chemical shifts are reported in ppm (δ) relative to TMS, referenced to the chemical shifts of residual solvent resonances (¹H). FT-IR spectra were recorded on a Perkin-Elmer FT-IR/Raman 2000 instrument in the transmission mode; samples were prepared as KBr disks (by mixing samples with spectroscopic grade KBr) and analyzed in the 400–4000 cm^{−1} range. Thermogravimetric analysis (TGA) data were recorded on a EXSTAR Thermo Gravimetric Analyzer (TG/DTA) Seiko 6200 under flowing air (50 mL/min) in the 40–500 °C temperature range using a heating ramp of 2 °C min^{−1}; TGA measurements have been conducted in order to estimate the average organic content of the synthesized Pd-nanoparticles. Transmission electron microscopy

(TEM) analyses were carried out with a JEM 3010 (JEOL) electron microscope operating at 300 kV, with point to point resolution at a Scherzer defocus of 0.17 nm. Samples for TEM analysis were transferred as a solution (in THF or MeOH) to a copper grid covered with a holey carbon film. Inductively coupled plasma–atomic emission spectroscopy (ICP-AES) analyses were conducted on a Spectroflame Modula E Optical Plasma Interface (OPI) instrument by SpectroTM. Gas chromatography–mass spectrometry (GC-MS) analyses were carried out on an Agilent 7890 GC mounting a J&W DB-225ms column (60 m, i.d. 0.25 mm, 250 μ m) and coupled with a Agilent 5975 MS.

2.2. Synthesis of MUA-Pd Nanoparticles. MUA nanoparticles were prepared by varying three synthetic parameters systematically, namely: (a) the temperature of the reduction step; (b) the thiol/Pd molar ratio; and (c) the addition rate of the reducing agent (NaBH₄). Except for TEM characterization (morphological characteristics of the differently prepared MUA-Pd nanoparticles), neither appreciable spectroscopic differences (NMR, FT-IR spectra) nor significant difference in the Pd/organic content ratio (TGA) were found in the nanoparticles prepared according to the different procedures outlined below.

(a). *Synthesis of MUA-Pd Nanoparticles at Different Temperatures of the Reduction Step (Thiol/Pd Molar Ratio = 0.5, Fast Addition of the Reducing Agent).* K₂PdCl₄ (20.0 mg) is first dissolved in 2 mL of water, and then 10 mL of acetone are added. To the red solution, H₃PO₄ (250 μ L, 60 mol vs Pd) is added, followed by 11-mercaptopundecanoic acid (MUA, 7.0 mg). MUA addition caused the color of the solution to change from red to red-yellowish. The solution is stirred for 5 min, and the reaction temperature is adjusted to one of the following values: 0, −50, or −78 °C (by means of ice, acetone/liquid N₂, or acetone/dry ice baths, respectively). Afterward, a freshly prepared aqueous solution (1 mL) of NaBH₄ (23.2 mg, 10 mol vs Pd) is rapidly added in one portion, causing the solution to turn immediately black. Stirring is continued at the reduction temperature for 5 min and at RT for other 5 min, and then solvents are evaporated under vacuum and the particles washed three times with dichloromethane (10 mL portions) and three times with water (10 mL portions), with sonication and centrifugation (4500 rpm, 10 min) after each washing cycle. Particles are then recovered by dissolution in THF.

(b). *Synthesis of MUA-Pd Nanoparticles at Different Thiol/Pd Molar Ratios (0 °C as Temperature of the Reduction Step, Fast Addition of the Reducing Agent).* K₂PdCl₄ (20.0 mg) is first dissolved in 2 mL of water, and then 10 mL of acetone are added. To the red solution, H₃PO₄ (250 μ L, 60 mol vs Pd) is added, followed by 11-mercaptopundecanoic acid in different amounts (MUA, 3.5 mg for 0.25 molar ratio or 10.5 mg for 0.75 molar ratio). MUA addition caused the solution color to change from red to red-yellowish. Temperature is adjusted to 0 °C by means of an ice bath, and then a freshly prepared aqueous solution (1 mL) of NaBH₄ (23.2 mg, 10 mol vs Pd) is added within 5 s, causing the solution to turn immediately black. Stirring is continued at 0 °C for 5 min and at RT for other 5 min, and then solvents are evaporated under vacuum and the particles washed three times with dichloromethane (10 mL portions) and three times with water (10 mL portions), with sonication and centrifugation (4500 rpm, 10 min) after each washing cycle. Particles are then recovered by dissolution in THF.

(c). *Synthesis of MUA-Pd Nanoparticles at Slow Rate Addition of the Reducing Agent (0 °C as Temperature of the Reduction Step, Thiol/Pd Molar Ratio = 0.5).* K₂PdCl₄ (20.0 mg) is first dissolved in 2 mL of water, and then 10 mL of acetone are added. To the red solution, H₃PO₄ (250 μ L, 60 mol vs Pd) is added, followed by 11-mercaptopundecanoic acid (MUA, 7.0 mg). MUA addition caused the solution color to change from red to red-yellowish. Temperature is adjusted to 0 °C by means of an ice bath, and then a freshly prepared aqueous solution (1 mL) of NaBH₄ (23.2 mg, 10 mol vs Pd) is added dropwise within 15 min, causing the solution to turn black after just 1 min. Stirring is continued at 0 °C for 5 min and at RT for other 5 min, and then solvents are evaporated under

vacuum and the particles washed three times with dichloromethane (10 mL portions) and three times with water (10 mL portions), with sonication and centrifugation (4500 rpm, 10 min) after each washing cycle. Particles are then recovered by dissolution in THF.

MUA-Pd nanoparticles characterization: ^1H NMR (CD_3OD , 298 K) δ : 1.38 (br, $-\text{CH}_2-$), 1.62 (br, $-\text{CH}_2\text{CH}_2\text{COOH}$), 2.30 (br, $-\text{CH}_2\text{COOH}$). IR (KBr) ν (cm^{-1}): 2926, 2853, 1710. TGA analysis has allowed the assessment of an average organic content of ca. 45 wt % for all samples prepared according to the procedures outlined above.

2.3. Synthesis of MUATE-Pd Nanoparticles. The procedure for the synthesis of 11-mercaptopundecanoate-functionalized Pd nanoparticles (MUATE-Pd) is identical to one of those described above for MUA-Pd nanoparticles (*room temperature of the reduction step, thiol/Pd molar ratio = 0.5, fast addition of the reducing agent*), except for the use of H_3PO_4 . Pd-nanoparticles precipitated out from the solution after addition of NaBH_4 and were washed with acetone (3×10 mL portions) and methanol (3×10 mL portions), with sonication and centrifugation (4500 rpm, 10 min) after each washing cycle. The as-prepared nanoparticles are completely soluble in water due to the presence of carboxylate groups which decorate their surface. ^1H NMR (D_2O , 298 K) δ : 1.30 (br, $-\text{CH}_2-$), 1.51 (br, $-\text{CH}_2\text{CH}_2\text{COOH}$), 2.14 (br, $-\text{CH}_2\text{COOH}$). IR (KBr) ν (cm^{-1}): 2917, 2847, 1555, 1399.

2.4. Synthesis of MN-Pd Nanoparticles. The procedure for the synthesis of 9-mercapto-1-nonanol-functionalized Pd nanoparticles (MN-Pd) is identical to one of those described above for MUA-Pd nanoparticles (*room temperature of the reduction step, thiol/Pd molar ratio = 0.5, fast addition of the reducing agent*), except for the use of MN instead of MUA. Pd-nanoparticles precipitated out from the solution after addition of NaBH_4 and were washed with THF (3×10 mL portions) and water (3×10 mL portions), with sonication and centrifugation (4500 rpm, 10 min) after each washing cycle. The as-prepared nanoparticles are completely soluble in methanol. ^1H NMR (CD_3OD , 298 K) δ : 1.36 (br, $-\text{CH}_2-$), 1.54 (br, $-\text{CH}_2\text{CH}_2\text{OH}$), 3.57 (br, $-\text{CH}_2\text{OH}$). IR (KBr) ν (cm^{-1}): 3417, 2918, 2847, 1235. TGA analysis has allowed the assessment of an average organic content of ca. 35 wt %.

2.5. Synthesis of DT-Pd Nanoparticles. The procedure for the synthesis of 1-dodecanethiol-functionalized Pd nanoparticles (DT-Pd) is identical to one of those described above for MUA-Pd nanoparticles (*room temperature of the reduction step, thiol/Pd molar ratio = 0.5, fast addition of the reducing agent*), except for the use of DT instead of MUA and $\text{H}_2\text{O}/\text{THF}$ (1/6 v/v) as solvent. Pd-nanoparticles precipitated out from the solution after addition of NaBH_4 and were washed with water (3×10 mL portions), methanol (3×10 mL portions), and acetone (3×10 mL portions), with sonication and centrifugation (4500 rpm, 10 min) after each washing cycle. The as-prepared nanoparticles are completely soluble in THF, CH_2Cl_2 , CHCl_3 , toluene, and alkanes. ^1H NMR (CDCl_3 , 298 K) δ : 0.88 (br, $-\text{CH}_3$), 1.26 (br, $-\text{CH}_2-$). IR (KBr) ν (cm^{-1}): 2918, 2847, 1451. TGA analysis has allowed the assessment of an average organic content of ca. 35 wt %.

2.6. Synthesis of Mixed-Monolayer Protected Pd Nanoparticles. The procedure for the synthesis of mixed-monolayer Pd nanoparticles is identical to one of those (single-component) described above for MUA-Pd nanoparticles (*room temperature of the reduction step, thiol/Pd molar ratio = 0.5, fast addition of the reducing agent*) except for the use of mixtures of thiols.

(a). **MUA-MN-Pd Nanoparticles.** K_2PdCl_4 (20.0 mg) is first dissolved in 2 mL of water, and then 10 mL of acetone are added. To the red solution, H_3PO_4 (250 μL , 60 mol vs Pd) is added, followed by MUA (3.5 mg, 0.25 mol vs Pd) and MN (3.0 μL , 0.25 mol vs Pd). The solution is stirred for 5 min, and then a freshly prepared aqueous solution (1 mL) of NaBH_4 (23.2 mg, 10 mol vs Pd) is rapidly added in one portion, causing the solution to turn immediately black. Stirring is continued at RT for 5 min, and then solvents are evaporated under vacuum and the particles washed three times with dichloromethane (10 mL portions)

and three times with water (10 mL portions), with sonication and centrifugation (4500 rpm, 10 min) after each washing cycle. The as-prepared nanoparticles were then recovered by dissolution in THF. Notably, these mixed-layer Pd-nanoparticles showed good solubility in both methanol and acetone. ^1H NMR (CD_3OD , 298 K) δ : 1.38 (br, $-\text{CH}_2-$), 1.59 (br, $-\text{CH}_2\text{CH}_2\text{OH}$, $-\text{CH}_2\text{CH}_2\text{COOH}$), 2.30 (br, $-\text{CH}_2\text{COOH}$), 3.57 (br, $-\text{CH}_2\text{OH}$). IR (KBr) ν (cm^{-1}): 3417, 2922, 2849, 1700.

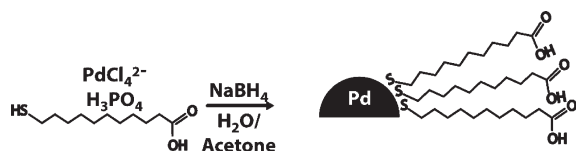
(b). **MUA-DT-Pd Nanoparticles.** The procedure used is identical to that described above for MUA-MN-Pd nanoparticles, except for the use of 3.0 mg of MUA (0.25 mol vs Pd) and 3.9 μL of DT (0.25 mol vs Pd) as mixture of thiols. In the present case, the final nanoparticles showed only moderate solubility in methanol and acetone while being completely soluble in THF. ^1H NMR (acetone- d_6 , 298 K) δ : 0.91 (br, $-\text{CH}_3$), 1.34 (br, $-\text{CH}_2-$), 1.61 (br, $-\text{CH}_2\text{CH}_2\text{COOH}$), 2.30 (br, $-\text{CH}_2\text{COOH}$). IR (KBr) ν (cm^{-1}): 2941, 2920, 2851, 1708.

(c). **MN-DT-Pd Nanoparticles.** The procedure used is identical to that described above for MUA-MN-Pd nanoparticles, except for the use of 3.0 μL of MN (0.25 mol vs Pd) and 3.9 μL of DT (0.25 mol vs Pd), as a mixture of thiols and $\text{H}_2\text{O}/\text{THF}$ (1/5 v/v) was used to dissolve the Pd precursor. In the present case the final nanoparticles showed good solubility only in THF. IR (KBr) ν (cm^{-1}): 3420, 2946, 2919, 2849, 1451.

2.7. Postfunctionalization of MUA-Pd Nanoparticles with Amine and Alcohols (1-Hexadecylamine, Benzylamine, and 1-Hexanol). MUA-Pd nanoparticles (20 mg) were dissolved in 10 mL of dry THF (<0.002% H_2O) and treated with 5 equiv (relative to the moles of MUA in the monolayer) of BOP, HOBT, NMM, and DMAP. After a brief activation time (10–15 min), either the amine (1-hexadecylamine or benzylamine, 5 equiv) or the alcohol (1-hexanol, 10 equiv) were added, and the system was maintained under stirring at room temperature overnight. Afterward, solvent was removed under vacuum, and the crude residue was purified by successive washing cycles with methanol (three times) and CH_3CN (three times) in order to remove all unreacted reagents and undesired byproducts. Postfunctionalized MUA-Pd-nanoparticles in the form of amido derivatives showed good solubility in DCM as well as other organic (less polar) solvents while ester derivatives (MUA-Pd reacted with 1-hexanol) showed good solubility also in THF. 1-Hexadecylamine-derivatized MUA-Pd nanoparticles: ^1H NMR (CDCl_3 , 298 K) δ : 0.87 (br, $-\text{CH}_3$), 1.24 (br, $-\text{CH}_2-$), 1.48 ($-\text{CH}_2-\text{CH}_2\text{CONH}$), 1.75 ($-\text{CH}_2-\text{CH}_2-\text{NHCO}$), 2.15 (br, $-\text{CH}_2\text{CONH}$), 3.19 (br, $-\text{CH}_2\text{NH}$). IR (KBr) ν (cm^{-1}): 3287, 2959, 2920, 2850, 1640, 1541. TGA analysis has allowed the assessment of an organic content of ca. 60 wt %. Benzylamine-derivatized MUA-Pd nanoparticles: ^1H NMR (CDCl_3 , 298 K) δ : 1.23 (br, $-\text{CH}_2-$), 1.57 ($-\text{CH}_2-\text{CH}_2\text{CO}$), 2.16 (br, $-\text{CH}_2\text{CONH}$), 4.34 (br, $-\text{CH}_2\text{NH}$), 7.22 (br, C_6H_5-). IR (KBr) ν (cm^{-1}): 3303, 2922, 2850, 1642, 1538. 1-Hexanol-derivatized MUA-Pd nanoparticles: ^1H NMR (CDCl_3) δ : 0.88 (br, $-\text{CH}_3$), 1.29 (br, $-\text{CH}_2-$), 1.66 ($-\text{CH}_2-\text{CH}_2\text{O}$), 2.27 (br, $-\text{CH}_2\text{COO}$), 4.05 (br, $-\text{CH}_2\text{O}$). IR (KBr) ν (cm^{-1}): 2924, 2852, 1735, 1451.

2.8. General Procedure for the Suzuki Cross-coupling Reactions using MUA-Pd Nanoparticles. To a hot (90 $^\circ\text{C}$) N,N -dimethylformamide (5 mL) solution of aryl halide (1.0 mmol), phenylboronic acid (1.3 mmol), NaOH (1.5 mmol), and naphthalene (0.5 mmol as internal standard), a THF solution (2 mL) of MUA-Pd nanoparticles (2 mg as Pd content) was added in one portion. The course of the reaction was monitored by GC-MS analysis using naphthalene as internal standard until complete reagents' consumption. After cooling the mixture to RT, 15 mL of CH_2Cl_2 and 15 mL of water were added. The collected organic phase was washed three times with H_2O (15 mL), dried over anhydrous sodium sulfate, and evaporated under reduced pressure to give the expected cross-coupling products. Chemical yields were determined from the crude

Scheme 1. Synthesis of the MUA-Pd Nanoparticles



materials by GC analysis (using naphthalene as internal standard), and cross-coupling products were analyzed by ^1H NMR (CDCl_3) spectroscopy and compared with literature data.^{22,23}

In the case of nanoparticle recycling and reuse, the reaction mixture underwent centrifugation cycles prior to the workup. Recovered nanoparticles were washed with toluene (3×5 mL), acetone (3×5 mL), methanol (3×5 mL), and water (3×5 mL); afterward, clean nanoparticles were recovered by dissolution in acidic THF and successfully reused as cross-coupling catalysts (MUA-Pd nanoparticle reuse in Suzuki cross-coupling did not show any significant activity loss even after three successive runs).

3. RESULTS AND DISCUSSION

3.1. Synthesis of MUA-Pd Nanoparticles. A simple and efficient protocol for the preparation of Pd nanoparticles stabilized by alkyl thiols containing either carboxylic [11-mercaptoundecanoic acid (MUA)] or hydroxyl [9-mercapto-1-nonanol (MN)] functional end-groups is proposed. Thiol-stabilized Pd nanoparticles featured by carboxylic functional end-groups at the edge of the self-assembled monolayer have been conveniently prepared starting from a water/acetone 1/5 (v/v) solution of K_2PdCl_4 and MUA in the presence of phosphoric acid in slight excess with respect to NaBH_4 . Afterward, the addition of NaBH_4 causes the almost instantaneous Pd^{II} reduction and the subsequent formation of mostly monodisperse (~ 2 nm) amphiphilic palladium nanoparticles (Scheme 1).

While the use of an aqueous reaction mixture guarantees a complete dissolution of the Pd^{II} precursor, acetone is essential to solvate the final Pd–thiol complex that is formed. Moreover, the complete miscibility of acetone and water (single phase) does not require the use of ammonium alkyls as phase transfer agents, thus reducing expensive and time-consuming purification procedures of the as-synthesized core–shell nanoparticles. Unlike related core–shell nanoparticles syntheses based on gold,²⁴ the use of methanol as a solvent turned out to be unsuitable in the case of palladium because of a rapid precipitation of Pd^{II} -thiol based species upon the simple addition of MUA thiol. Most importantly, the use of an excess of phosphoric acid turned out to be crucial for the successful synthesis of the MUA Pd-nanoparticles; indeed, while preventing thiol and carboxylic acid deprotonation in the single phase reduction step (addition of NaBH_4), it maintains the $\text{Pd}(\text{II}) \rightarrow \text{Pd}(0)$ reductive path highly competitive with respect to other possible acid–base side reactions. As a matter of fact, a slight excess of NaBH_4 with respect to Pd is needed to drive the reduction process to completeness. Once MUA-Pd nanoparticles are formed, the NaBH_4 residue is rapidly consumed by the excess of phosphoric acid, thus protecting the carboxylic groups at the edge of the SAM from undesirable deprotonation/reduction side processes.

Notably, the MUA-Pd core–shell nanoparticles are straightforwardly isolated in their purified form after simple washing/centrifugation treatments, using in sequence: (a) CH_2Cl_2 , to

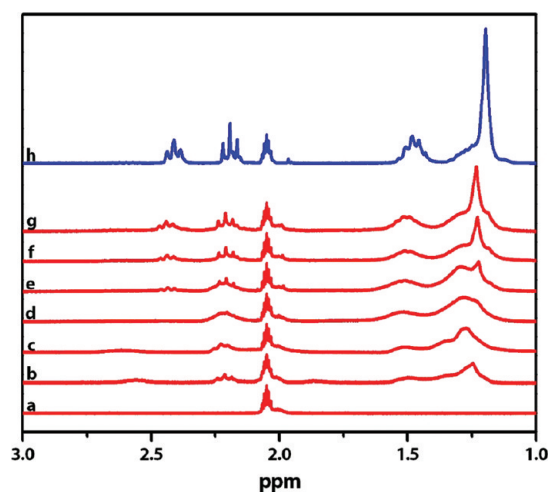


Figure 1. ^1H NMR spectra of K_2PdCl_4 solutions (in D_2O /acetone- d_6 1:5 v/v) after the addition of (a) 0 mol equiv, (b) 0.5 mol equiv, (c) 1.0 mol equiv, (d) 1.5 mol equiv, (e) 2.0 mol equiv, (f) 2.5 mol equiv, and (g) 3.0 mol equiv of MUA. (h) MUA ^1H NMR spectrum in D_2O /acetone- d_6 1:5 v/v.

remove the unreacted thiol, and (b) water to eliminate all the inorganic side-products. Neither precipitation/dissolution cycles using acids or bases²⁰ nor additional purification protocols are needed to get purified nanoparticles. Accordingly, this synthetic protocol offers an easy and convenient approach to the nanoparticle synthesis scale-up (up to 500 mg of MUA-Pd nanoparticles).

The resulting MUA-Pd nanoparticles are highly soluble in organic polar (protic and aprotic) solvents such as methanol, acetone, DMF, and THF in high concentrations (up to 10 mg/mL) while they are insoluble in CH_2Cl_2 and water.

Three synthetic parameters (reaction temperature, thiol/Pd molar ratio, and rate of reductant addition) have been systematically scrutinized in order to elucidate their influence on the final Pd nanoparticle size distribution, and they are discussed hereafter.

3.2. Involvement of Pd-thiolate Species as Precursors. ^1H NMR spectroscopy (in D_2O /acetone- d_6 1/5 at 298 K) was exploited to shed light on the MUA-Pd nanoparticle synthesis. As Figure 1 shows, the successive addition of the thiol carboxylic acid (MUA) to a K_2PdCl_4 solution (0.5, 1.0, and 1.5 mol equiv of MUA) results in the appearance of a triplet around 2.30 ppm, assigned to the methylene groups vicinal to the COOH moiety. Notably, the methylene protons vicinal to the SH group remain almost invisible up to the addition of 2 mol equiv of the thiol. Such an effect has been attributed to the interaction of the SH groups with the Pd^{II} centers; in fact, a signal broadening of the methylene protons vicinal to the SH group is expected until complete saturation of the Pd^{II} coordination sphere. Indeed, a new broad triplet around 2.4 ppm starts to appear after the addition of an excess of thiol (over 2 mol equiv), ultimately suggesting that mercapto-groups prevalently contribute to the composition of the Pd^{II} coordination sphere in solution.

Accordingly, one may conclude that the Pd^{II} -thiolate species are formed with a 1:2 stoichiometry ($\text{Pd}^{\text{II}}/\text{MUA}$), very likely in the form of oligomeric species (from the broadening of ^1H NMR signals).¹⁴ FT-IR spectroscopy data are in line with the NMR investigation. Indeed, only a very weak and broad band around

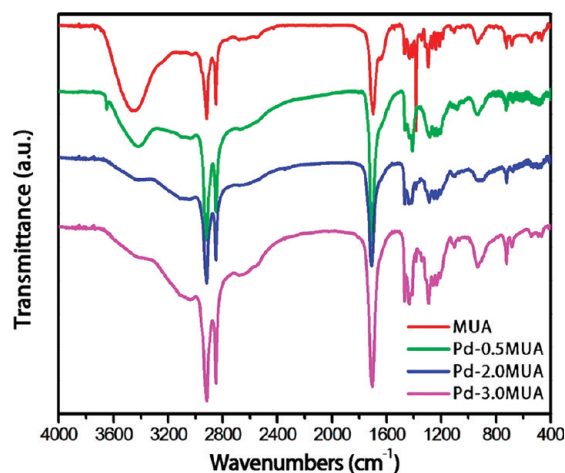


Figure 2. FT-IR spectra of MUA and K_2PdCl_4 in the presence of different amounts of MUA (0.5, 2.0, and 3.0 mol equiv).

2530 cm^{-1} (attributed to the stretching mode of the S–H groups of the MUA) appears at high MUA/Pd molar ratios ($\approx 3/1$), while no appreciable changes of the intense stretching mode attributed to the carboxylic C=O bond are observed (Figure 2). All these data taken together offer clear evidence that Pd^{II} -thiolate species are the precursors of the Pd NPs bearing carboxylic groups at the edge of the SAM. On this basis, metal–thiolate species can also be taken as useful precursors for the preparation of nanoparticles with single phase methods.²⁵

3.3. Effect of Reaction Parameters on the Size of MUA-Pd Nanoparticles: TEM Characterization. Three synthetic parameters (reaction temperature, thiol/Pd molar ratio, and rate of reductant addition) have been systematically scrutinized in order to elucidate their influence on the final Pd nanoparticle size distribution. Overall, MUA-Pd nanoparticles size and NPs size distributions appear to be moderately influenced by variations of the first two parameters (reaction temperature and thiol/Pd molar ratio), while the very fast reduction of Pd^{II} to Pd^0 upon treatment with NaBH_4 seems to be the most relevant issue for the nanoparticle size control.

Figure 3a shows the morphological characterization (TEM) of the MUA-Pd nanoparticles prepared upon rapid addition of the reducing agent to a room temperature solution of K_2PdCl_4 and MUA in a 0.5 thiol/Pd molar ratio. Notably, this protocol provides nanoparticles featured by rather small metal cores and a narrow size distribution ($1.9 \pm 0.2\text{ nm}$, Figure 4, panel A). TEM micrographs show large patches on the TEM grid (Figure S2 of the Supporting Information) due to the presence of a high nanoparticle density, most likely interacting with one another through the respective carboxylic groups. In spite of that, the protonation of the carboxylic groups maintains the nanoparticles well separated in solution, while Pd-agglomerates rapidly form in organic solvents by simple treatment with a base (COOH deprotonation and formation of MUAte-Pd). It should be pointed out that related Au nanoparticles⁹ show the opposite behavior, leading to nanoparticle agglomerates under acidic conditions.

Only negligible variations on the average size of Pd-NPs cores were observed while decreasing the reduction temperature from RT to 0, -50 , and $-78\text{ }^\circ\text{C}$, respectively (maintaining constant the thiol/Pd molar ratio at 0.5, with a rapid addition of the reducing agent) (Figures 3b and 4, panel A). However, an

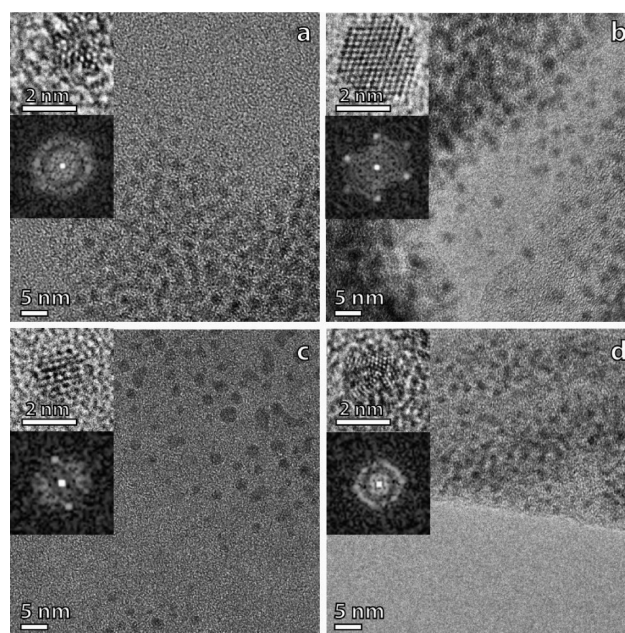


Figure 3. Representative TEM micrographs of MUA-Pd nanoparticles obtained using different experimental conditions. (a) RT, thiol/Pd 0.5, fast reductant addition; (b) $-78\text{ }^\circ\text{C}$, thiol/Pd 0.5, fast reductant addition; (c) $0\text{ }^\circ\text{C}$, thiol/Pd 0.75, fast reductant addition; (d) $0\text{ }^\circ\text{C}$, thiol/Pd 0.5, slow reductant addition. Insets: representative HRTEM images of single Pd nanoparticles (top left of each figure) and their corresponding Hanning masked fast Fourier transformations (FFTs, bottom).

in-depth high-resolution TEM (HRTEM) investigation (Figure S3 of the Supporting Information) showed that the lower the reduction temperature, the higher the Pd-NPs crystallinity (see inset in Figure 3a vs inset in Figure 3b). This trend is likely due to a slower particles growth rate once the initial NPs-nuclei are generated; as a consequence, a better packing of the Pd atoms during the nanoparticle formation process is expected. Accordingly, MUA-Pd nanoparticles synthesis at high temperature (i.e., addition of the reducing agent at $65\text{ }^\circ\text{C}$) leads to small Pd-NPs (around 1.5 nm) featured by highly disordered structures (Figure S4 of the Supporting Information).

The inset in Figure 3b shows a particle imaged at Scherzer defocus oriented along the $\langle 101 \rangle$ zone axis,²⁶ and it demonstrates the crystallinity of the as-prepared nanoparticles with interplanar distances of 0.22 and 0.19 nm , in accordance with the $\{111\}$ and $\{200\}$ crystallographic planes of the Pd metal, respectively; most of the crystalline nanoparticles present a cuboctahedral shape.

Only moderate differences in both nanoparticle size and distribution were observed upon varying the MUA/Pd molar ratio while maintaining the other two parameters constant ($0\text{ }^\circ\text{C}$, fast addition of the reducing agent) (Figure 3c and 4, panel B). As Figure 4 (panel B) shows, high thiol/Pd molar ratios lead to smaller particle sizes and narrower size distributions (Figure 4, panel B). While a higher thiol/Pd molar ratio is found to decrease the NPs growth rate, their nucleation rate is almost unaffected.

Finally, the effect of the reductant addition rate has also been investigated. Unlike alkanethiol-protected Au nanoparticles,²⁷ a slow addition of the reducing agent did not appreciably change the Pd-NPs size distribution, although a large population of small nanoparticles ($<1.8\text{ nm}$) was formed (Figure 3d and 4, panel C). Such a result is likely due to a most favored nucleation process as a consequence of a slow addition of the reducing agent.

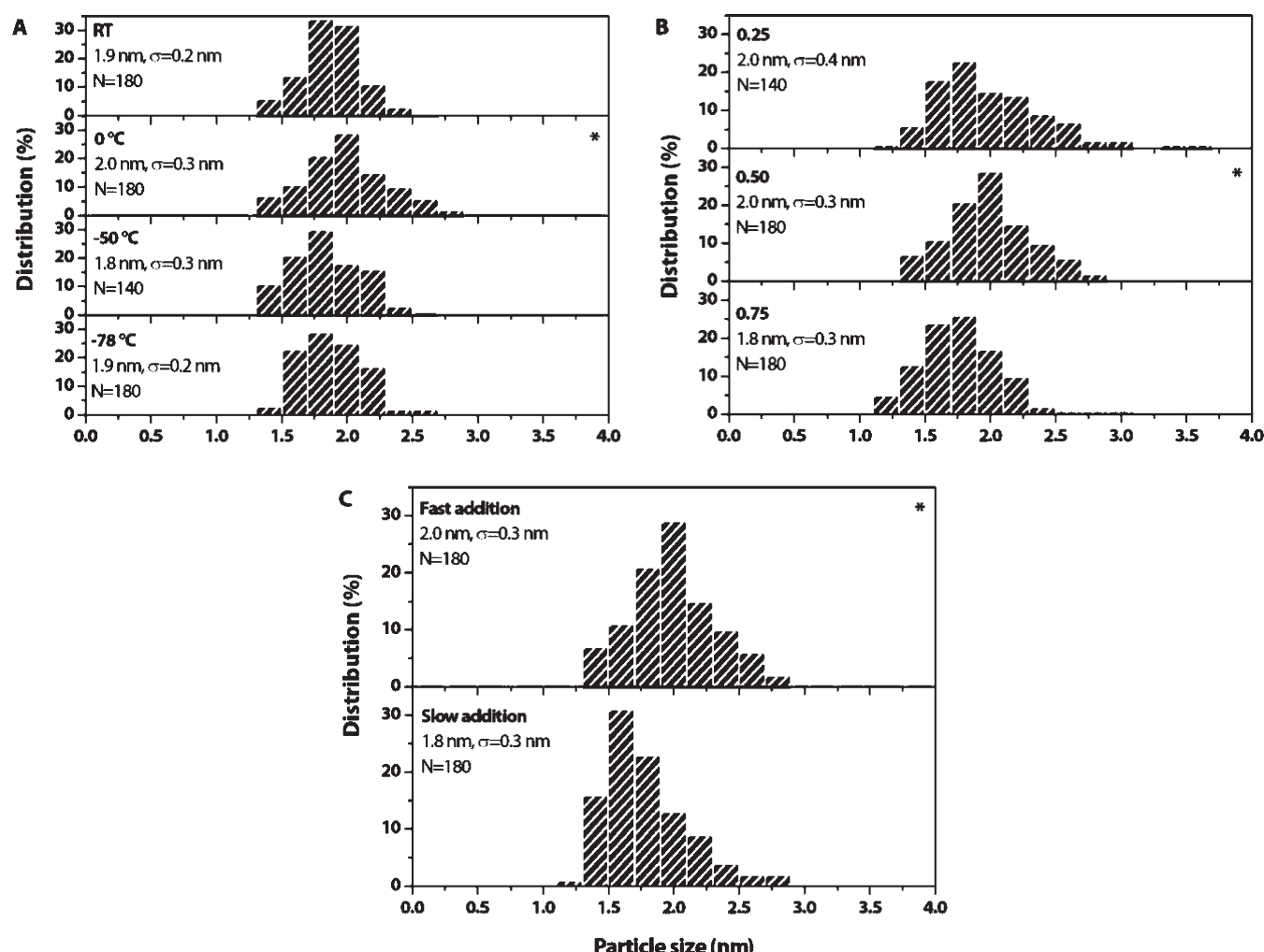


Figure 4. Particle size distributions of MUA-functionalized Pd nanoparticles prepared under different conditions: panel A refers to the effect of temperature (RT: room temperature); panel B refers to the effect of thiol/Pd molar ratio; panel C refers to the effect of addition rate of the reducing agent (NaBH_4) (fast, 10 s; slow, 15 min). Average particle size, dispersions (σ , in nm), and number of counted particles (N) are also reported. Asterisks denote size distributions under the same reaction conditions.

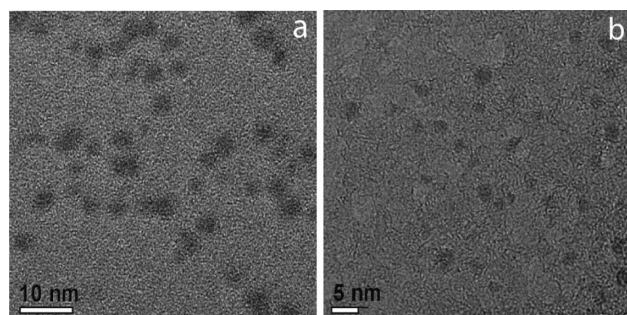


Figure 5. Representative TEM images of MN-Pd (a) and DT-Pd (b) nanoparticles prepared at room temperature (reduction step) and thiol/Pd molar ratio = 0.5, with fast addition of the reducing agent.

Since the average size of MUA-Pd NPs appears to be mainly controlled by the very fast metal reduction upon addition of NaBH_4 (reaction temperature and thiol/Pd molar ratio were found to influence the NPs size only marginally), the role of these synthetic parameters was no longer investigated in the case of Pd-NPs stabilized with different thiols.

3.4. Synthesis of MUAte-, MN-, DT-, and Mixed-Monolayer Pd Nanoparticles. Pd-nanoparticles featuring a high density of carboxylate functional groups at the edge of the single monolayer have been conveniently prepared from the procedure outlined above for MUA-Pd nanoparticles, except for the use of phosphoric acid. Indeed, the absence of the strong acid leads to carboxylic acid deprotonation upon simple addition of the reducing agent, followed by rapid nanoparticle precipitation. Notably, the as-prepared carboxylate Pd-nanoparticles (MUAte-Pd), which are protected against undesired agglomeration effects by the formation of a double layer of negative and positive charges, present high solubility in water (physiological conditions at pH 7.4) up to 10 mg of Pd per milliliter of solvent. Such a result is of major importance in light of their potential use in biological applications.

Aimed at highlighting the extremely high versatility of this protocol, the synthetic procedure used for the preparation of MUA-Pd nanoparticles was successfully applied (with only minor changes) to other functionalized or simply alkyl thiols such as the 9-mercapto-1-nonanol (MN) and the 1-dodecanethiol (DT). DT-Pd nanoparticles were prepared in a mixture of THF/ H_2O (instead of acetone/ H_2O) in order to ensure the

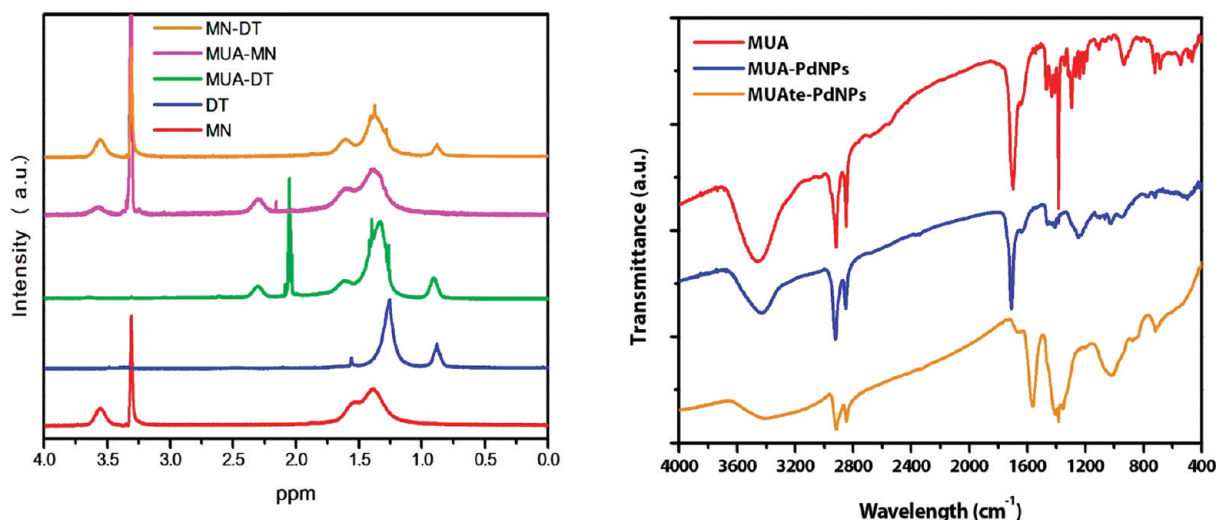


Figure 6. (left) ¹H NMR spectra of MN-Pd (in CD₃OD), DT-Pd (in CDCl₃), MUA-DT (in acetone-*d*₆), MUA-MN (in CD₃OD), and MN-DT nanoparticles (in CD₃OD). (right) FT-IR spectra of free MUA, MUA-Pd nanoparticles, and MUAt-Pd nanoparticles (KBr pellets).

solubility of the thiol-Pd^{II} species formed upon DT addition to a solution of K₂PdCl₄. The final DT-Pd nanoparticles are soluble in organic solvents such as THF, DCM, toluene, and alkanes, while nanoparticles bearing hydroxyl functional groups at their edges (MN-Pd) show high solubility in methanol. The versatility of this protocol is further evidenced by the possibility of preparing mixed-monolayer protected Pd nanoparticles. By simple changes in the reaction conditions (i.e., the mixture of reagents), MUA-MN, MUA-DT, and MN-DT Pd nanoparticles were prepared, where the two different thiols (in a roughly 1/1 molar ratio) were brought on the nanoparticle board. Unlike “place-exchange” reaction protocols⁸ (where the production of mixed monolayers is severely limited by the equilibrium character of the process), the presented methodology allows for a fine-tuning of functional groups density decorating the nanoparticle surface, as well as a facile control of the nature of the functional groups in the mixed monolayers. Figure 5 shows two representative TEM images of the MN-Pd (a) and DT-Pd (b) nanoparticles, respectively. Both samples present similar nanoparticle distributions to those observed for the MUA-Pd sample with an average nanoparticles diameter of ~2 nm. In the case of nanoparticles stabilized by mixed monolayers, TEM images have finally revealed the presence of similar nanoparticles (average diameter of ~2 nm), although small metal clusters are also present throughout the whole scanned area (Figure S5 of the Supporting Information).

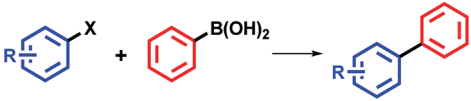
The ¹H NMR spectra of the MN- and DT-Pd nanoparticles show almost similar patterns to the MUA-Pd one, featured by the absence of clear resonances from the methylene groups vicinal to sulfur atoms and broadened signals for all other methylene moieties (Figure 6, left). While signals around 3.6 ppm in the MN-Pd NPs ¹H NMR spectrum have been unequivocally attributed to the hydroxyl vicinal methylene groups, the resonance around 0.8 ppm in the DT-Pd NPs ¹H NMR spectrum reasonably belongs to the terminal methyl groups of the thiol alkyl chains.²⁸

In the case of the mixed-monolayer Pd nanoparticles, the ¹H NMR spectra clearly demonstrate that both thiols are present in the monolayer (Figure 6, left). Most importantly, the initial thiols molar ratio is entirely maintained in the final nanoparticles

monolayer composition, as evidenced by the integrals of the characteristic resonances unequivocally assigned to the two thiols. Though the classical I₂ decomposition method²⁸ for the quantitative estimation of the monolayer composition can be applied to particles protected by alkyl thiols, we found that when the acidic groups are present in the monolayer, this procedure failed to give quantitative results. Nevertheless, the estimation of the monolayer composition based on the signals of the groups far from the metal core has been conveniently applied in our case.

FT-IR spectroscopy has also been applied to the characterization of the NPs monolayer composition. As Figure 6 (right) shows, the most relevant difference among the IR spectra of MUA-Pd, MUAt-Pd nanoparticles, and free MUA is represented by a slight shift of the ν(C=O) vibrational mode. Indeed, the carboxylic groups of the MUA-Pd NPs show a shift of the ν(C=O) mode (compared to the free-MUA) of about +13 cm⁻¹, while a red-shift (compared to the free thiol) is observed for the MUAt-Pd NPs (1563 cm⁻¹). Minor shifts attributed to the symmetric (MUA-Pd 2853 cm⁻¹; MUAt-Pd 2848 cm⁻¹; MUA 2849 cm⁻¹) and antisymmetric (MUA-Pd 2926 cm⁻¹; MUAt-Pd 2918 cm⁻¹; MUA 2919 cm⁻¹) C–H stretching modes suggest the presence of *gauche* defects in the monolayer packing²⁷ caused by intermonolayer hydrogen bonding between adsorbed MUA molecules. FT-IR spectra of MN- and DT-Pd nanoparticles do not show a relevant difference from those reported for MUA-Pd NPs (Figure S6 of the Supporting Information).

Thermogravimetric analysis conducted on the MUA-Pd nanoparticles (Figure S7 of the Supporting Information) has revealed an organic content of about 45 wt %. This value, higher than that typically measured in the case of Au-based nanoparticles of similar size,²⁷ well fits with previous observations related to alkanethiol-protected Pd nanoparticles.¹⁴ Such an increased organic/metal ratio in the Pd NPs can be ascribed to several reasons: (a) the presence of subnanometer particles not clearly visible with a conventional TEM microscopy technique (due to the poor TEM contrast of Pd nanoparticles compared with Au ones²⁹), (b) the reduced Pd atomic radius compared to Au, and (c) the presence of residual tiara Pd^{II} thiolate complexes (Pd–thiol staple motifs),³⁰ as observed also for Au-based

Table 1. Suzuki Cross-Coupling Reactions Catalyzed by MUA-Pd Nanoparticles^a


entry	R	X	t (h)	yield ^b (%)
1	H	I	8	>99
2	4-CH ₃ CO	I	2	>99
3	2-CH ₃	I	4	98 ^c
4	H	Br	12	92
5	4-CH ₃ CO	Br	4	>99
6	4-CN	Br	1	>99
7	4-NO ₂	Cl	12	91

^a Reaction conditions: 1.0 mmol of aryl halide, 1.3 mmol of phenylboronic acid, 1.5 mmol of NaOH, MUA-Pd nanoparticles (2 mol % as Pd), 5 mL of *N,N*-dimethylformamide (DMF), 90 °C. ^b Reaction yields are determined by gas chromatography–mass spectrometry (GC-MS) analysis using naphthalene as internal standard. ^c Reaction yield >99% after 8 h.

systems.³¹ In the case of MN and DT-Pd NPs, an organic content of about 35 wt % was obtained, which can be due to slightly larger average diameters of the as-synthesized nanoparticles (Figures S8 and S9 of the Supporting Information).

3.5. Reactivity of MUA-Pd Nanoparticles. MUA-Pd nanoparticles have been investigated with respect to the reactivity of the carboxylic groups at the edge of the monolayer, using selected amidation and/or esterification protocols; such an approach paved the way to the preparation of complex molecular architectures directly at the nanoparticles surface.^{32,33} As for the MUA-Pd NPs, amidation was conducted in the presence of either 1-hexadecylamine or benzylamine,³⁴ while the ester derivative was prepared by reaction with 1-hexanol;³⁵ in both cases, the carboxylic acid activation was conveniently achieved according to literature procedures. As a result, both postfunctionalized MUA-Pd NPs showed enhanced solubility in polar and apolar organic solvents such as CH₂Cl₂, CHCl₃, and toluene, ultimately confirming the occurrence of an extensive monolayer derivatization. ¹H NMR and FT-IR spectra (Figures S10–S12 of the Supporting Information) have unambiguously demonstrated the high derivatization degree and the presence of amido and ester groups throughout the nanoparticle surface. Finally, the thermogravimetric analysis conducted on 1-hexadecylamine-derivate nanoparticles (Figure S13 of the Supporting Information) has shown a slightly higher organic content (60%) compared with that measured on pristine MUA-Pd NPs; this result fits well with an almost complete derivatization of the original carboxylic groups present at the surface of the NP monolayer.

3.6. Catalytic Activity of MUA-Pd Nanoparticles. The successful applicability of MUA-Pd nanoparticles as heterogeneous catalysts in combination with ceria as support has recently emerged in a number of fundamental chemical transformations, from CO oxidation to water-gas shift (WGS) and methanol steam re-forming (MSR) reactions.¹⁵ In addition, Hyeon and co-workers have shown the use of polymer protected Pd NPs in Suzuki cross-coupling reactions,¹¹ and Astruc and co-workers have also demonstrated that dodecanethiol-protected Pd nanoparticles are active heterogeneous catalysts

Table 2. Recycling Cycles for Suzuki Cross-coupling Reactions Catalyzed by MUA-Pd Nanoparticles^a

substrate/yield (%)	1st	2nd	3rd	4th	5th
iodobenzene	>99	98	98	97	98
4-bromobenzonitrile	>99	98	98	98	95

^a Reaction conditions: 1.0 mmol of aryl halide, 1.3 mmol of phenylboronic acid, 1.5 mmol of NaOH, MUA-Pd nanoparticles (2 mol % as Pd), 5 mL of *N,N*-dimethylformamide (DMF), 90 °C. Reaction time: 8 h for iodobenzene, 1 h for 4-bromobenzonitrile.

for the same cross-coupling reaction.³⁶ Suzuki cross-couplings are generally carried out using relatively large amounts of expensive Pd salts or organopalladium complexes, which are often difficult to recycle and need inert or controlled reaction atmospheres.³⁷ In order to overcome this problem, we were interested in evaluating the catalytic properties of our MUA-Pd NPs (prepared as follows: *room temperature of the reduction step, thiol/Pd molar ratio = 0.5, fast addition of the reducing agent*) as versatile, easily handled, and reusable heterogeneous catalysts for Suzuki cross-couplings. A selection of the catalytic results for cross-coupling reactions carried out with our MUA-Pd nanoparticles under literature conditions¹² is listed in Table 1.

Under basic reaction conditions, the NPs are present in their carboxylate form and can be easily recovered and separated from the reaction mixture already at room temperature. Once the mixture is heated at 90 °C, the MUate-Pd nanoparticles show excellent catalytic performances in the cross-coupling reaction of phenylboronic acid with several aryl halides. Reactions with iodide precursors are generally faster than those with bromides (Table 1, entries 1, 2, and 3 vs 4, 5, and 6), leading to almost quantitative substrate conversions even in the case of more sterically hindered aryl halides (entries 3 and 6). The reaction with the less reactive 4-nitrochlorobenzene (entry 7) has been used to widen the applicability of our protocol as well as to complete a general reactivity trend of the aryl halides under cross-coupling conditions (Aryl-I > Aryl-Br > Aryl-Cl). For all cases scrutinized, almost undetectable amounts (<1%) of the phenylboronic acid homocoupling byproduct were identified in the GC traces of the reaction mixture. These results are even more important in light of the very simple reaction conditions used (no oxygen-free conditions and solvents are required), the catalyst handiness, and its facile and complete recovery at the end of the catalytic process (through a simple centrifugation of the precipitated Pd NPs from the reaction mixture). Accordingly, NPs recovery and reuse cycles have been studied in the Suzuki cross-coupling protocol using either iodobenzene (Table 1, entry 1) or 4-bromobenzonitrile (Table 1, entry 6) as model aryl halides. Table 2 lists the catalytic performances of our MUA-Pd nanoparticles in terms of reaction yields, as obtained from their recycling in five successive cross-coupling protocols.

Only a slight decrease of the catalytic activity was observed in the first five cycles, indicating the high stability of the Pd NPs as catalyst for the Suzuki cross-coupling reaction. It seems that little differences (yield decrease) among the successive catalytic cycles are due to a partial catalyst loss during the centrifugation/washing treatment (NPs recycling). Remarkably, MUA-Pd nanoparticles can be isolated and redissolved (by acid treatment) after each cycle, with no appreciable loss of their catalytic performance throughout the whole recycling tests.

Pd leaching was assessed for each catalytic cycle by ICP analysis of the metal content in the crude reaction mixtures after the NPs removal by centrifugation; the amount of leached palladium was found to be absolutely negligible for each run (<1 ppm).

4. CONCLUSIONS

In this paper we have described a simple and highly efficient procedure for the large scale synthesis of differently functionalized thiol-protected Pd nanoparticles with rather small average NPs diameter and narrow NPs size distribution. MUA-Pd nanoparticles (~2 nm) have amphiphilic nature, because they are soluble in both organic solvents, when the functional group at the edge of the SAM is present in its protonated form, and water when it is deprotonated (carboxylates). A systematic study of the synthetic conditions applied to the NPs production (reaction temperature, thiol/Pd molar ratio, and reductant addition rate) as well as their morphological outcome has been properly addressed. The optimized synthetic protocol has also been applied to the preparation of hydroxyl functionalized nanoparticles (MN-Pd) and alkyl Pd nanoparticles (DT-Pd). Thiol mixtures have been finally used to prepare mixed-monolayer stabilized Pd nanoparticles with tunable properties, while easy derivatization protocols have been successfully applied to the MUA-Pd NPs for the preparation of ester- or amido-substituted NP monolayers. MUA-Pd nanoparticles have been finally scrutinized as highly efficient, easily handled, and reusable catalysts for Suzuki cross-coupling reaction with different aryl halides.

■ ASSOCIATED CONTENT

S Supporting Information. Additional representative TEM images and TGA, ¹H NMR, and FT-IR data. This material is available free of charge via the Internet at <http://pubs.acs.org>.

■ AUTHOR INFORMATION

Corresponding Author

*E-mail: pfornasiero@units.it.

■ ACKNOWLEDGMENT

Professor Mauro Graziani (University of Trieste) is kindly acknowledged for helpful discussions. Dr. Matteo Crosera and Professor Gianpiero Adami (University of Trieste) are kindly acknowledged for ICP analysis. University of Trieste, Università Ca' Foscari Venezia, Fondo Trieste, and Regione Friuli Venezia Giulia are acknowledged for financial support. R.J.G. and N.W. acknowledge support from AFOSR (MURI), Grant No. FA9550-08-1-0309.

■ REFERENCES

- (1) Daniel, M. C.; Astruc, D. *Chem. Rev.* **2004**, *104*, 293.
- (2) Love, J. C.; Estroff, L. A.; Kriebel, J. K.; Nuzzo, R. G.; Whitesides, G. M. *Chem. Rev.* **2005**, *105*, 1103.
- (3) Giljohann, D.; Seferos, D.; Daniel, W.; Massich, M.; Patel, P.; Mirkin, C. *Angew. Chem., Int. Ed.* **2010**, *49*, 3280.
- (4) Bianchini, C.; Shen, P. K. *Chem. Rev.* **2009**, *109*, 4183.
- (5) Jin, R.; Qian, H.; Wu, Z.; Zhu, Y.; Zhu, M.; Mohanty, A.; Garg, N. *J. Phys. Chem. Lett.* **2010**, *1*, 2903.
- (6) Brust, M.; Walker, M.; Bethell, D.; Schiffrin, D. J.; Whyman, R. *J. Chem. Soc., Chem. Commun.* **1994**, 801.
- (7) Roth, P. J.; Theato, P. *Chem. Mater.* **2008**, *20*, 1614.
- (8) Hostetler, M. J.; Templeton, A. C.; Murray, R. W. *Langmuir* **1999**, *15*, 3782.
- (9) Simard, J.; Briggs, C.; Boal, A. K.; Rotello, V. M. *Chem. Commun.* **2000**, 1943.
- (10) Sardar, R.; Shumaker-Parry, J. S. *Chem. Mater.* **2009**, *21*, 1167.
- (11) Piao, Y.; Jang, Y.; Shokouhimehr, M.; Lee, I. S.; Hyeon, T. *Small* **2007**, *3*, 255.
- (12) Rowe, M. P.; Plass, K. E.; Kim, K.; Kurdak, C.; Zellers, E. T.; Matzger, A. J. *Chem. Mater.* **2004**, *16*, 3513.
- (13) Yee, C. K.; Jordan, R.; Ulman, A.; White, H.; King, A.; Rafailovich, M.; Sokolov, J. *Langmuir* **1999**, *15*, 3486.
- (14) Zamborini, F. P.; Gross, S. M.; Murray, R. W. *Langmuir* **2001**, *17*, 481.
- (15) Cargnello, M.; Wieder, N. L.; Montini, T.; Gorte, R. J.; Fornasiero, P. *J. Am. Chem. Soc.* **2010**, *132*, 1402.
- (16) Kanaras, A. G.; Kamounah, F. S.; Schaumburg, K.; Kiely, C. J.; Brust, M. *Chem. Commun.* **2002**, 2294.
- (17) Templeton, A. C.; Chen, S.; Gross, S. M.; Murray, R. W. *Langmuir* **1998**, *15*, 66.
- (18) Cliffl, D. E.; Zamborini, F. P.; Gross, S. M.; Murray, R. W. *Langmuir* **2000**, *16*, 9699.
- (19) Pengo, P.; Polizzi, S.; Battagliarin, M.; Pasquato, L.; Scrimin, P. *J. Mater. Chem.* **2003**, *13*, 2471.
- (20) Chen, S.; Kimura, K. *Langmuir* **1999**, *15*, 1075.
- (21) Huang, X.; Wang, Y.; Liao, X.; Shi, B. *Chem. Commun.* **2009**, 4687.
- (22) Wolfe, J. P.; Singer, R. A.; Yang, B. H.; Buchwald, S. L. *J. Am. Chem. Soc.* **1999**, *121*, 9550.
- (23) Okamoto, K.; Akiyama, R.; Kobayashi, S. *Org. Lett.* **2004**, *6*, 1987.
- (24) Laaksonen, T.; Ahonen, P.; Johans, C.; Kontturi, K. *ChemPhysChem* **2006**, *7*, 2143.
- (25) Qian, H.; Jin, R. *Chem. Mater.* **2011**, *23*, 2209.
- (26) Ascencio, J. A.; Gutiérrez-Wing, C.; Espinosa, M. E.; Marín, M.; Tehuacanero, S.; Zorrilla, C.; José-Yacamán, M. *Surf. Sci.* **1998**, *396*, 349.
- (27) Hostetler, M. J.; Wingate, J. E.; Zhong, C. J.; Harris, J. E.; Vachet, R. W.; Clark, M. R.; Londono, J. D.; Green, S. J.; Stokes, J. J.; Wignall, G. D.; Glish, G. L.; Porter, M. D.; Evans, N. D.; Murray, R. W. *Langmuir* **1998**, *14*, 17.
- (28) Shon, Y. S.; Mazzitelli, C.; Murray, R. W. *Langmuir* **2001**, *17*, 7735.
- (29) Weir, M. G.; Knecht, M. R.; Frenkel, A. I.; Crooks, R. M. *Langmuir* **2009**, *26*, 1137.
- (30) Yang, Z.; Smetana, A. B.; Sorensen, C. M.; Klabunde, K. J. *Inorg. Chem.* **2007**, *46*, 2427.
- (31) Jadzinsky, P. D.; Calero, G.; Ackerson, C. J.; Bushnell, D. A.; Kornberg, R. D. *Science* **2007**, *318*, 430.
- (32) Zamborini, F. P.; Hicks, J. F.; Murray, R. W. *J. Am. Chem. Soc.* **2000**, *122*, 4514.
- (33) Abad, J. M.; Mertens, S. F. L.; Pita, M.; Fernandez, V. M.; Schiffrin, D. J. *J. Am. Chem. Soc.* **2005**, *127*, 5689.
- (34) Templeton, A. C.; Hostetler, M. J.; Warmoth, E. K.; Chen, S.; Hartshorn, C. M.; Krishnamurthy, V. M.; Forbes, M. D. E.; Murray, R. W. *J. Am. Chem. Soc.* **1998**, *120*, 4845.
- (35) McCafferty, D. G.; Bishop, B. M.; Wall, C. G.; Hughes, S. G.; Mecklenberg, S. L.; Meyer, T. J.; Erickson, B. W. *Tetrahedron* **1995**, *51*, 1093.
- (36) Lu, F.; Ruiz, J.; Astruc, D. *Tetrahedron Lett.* **2004**, *45*, 9443.
- (37) Moncada, A. I.; Manne, S.; Tanski, J. M.; Slaughter, L. M. *Organometallics* **2005**, *25*, 491.